Atmos. Chem. Phys. Discuss., 15, 24623–24642, 2015
www.atmos-chem-phys-discuss.net/15/24623/2015/
doi:10.5194/acpd-15-24623-2015

Atmospheric Chemistry and Physics Discussions
Open Access

Why does surface ozone peak before a typhoon landing in southeast China?

Y. C. Jiang[1], T. L. Zhao[1], J. Liu[2,3], X. D. Xu[4], C. H. Tan[1], X. H. Cheng[5], X. Y. Bi[6,7], J. B. Gan[8], J. F. You[9], and S. Z. Zhao[10]

[1]Collaborative Innovation Center on Forecast and Evaluation of Meteorological Disasters, Key Laboratory for Aerosol–Cloud-Precipitation of China Meteorological Administration, Nanjing University of Information Science and Technology, Nanjing 210044, China
[2]School of Atmospheric Sciences, Nanjing University, Nanjing 210093, China
[3]University of Toronto, Toronto, Ontario, M5S 3G3, Canada
[4]State Key Laboratory of Severe Weather, Chinese Academy of Meteorological Sciences, Beijing 100081, China
[5]Institute of Atmospheric Composition, Key Laboratory of Atmospheric Chemistry of China Meteorological Administration, Chinese Academy of Meteorological Sciences, Beijing 100081, China
[6]State Key Laboratory of Atmospheric Boundary Layer Physics and Atmospheric Chemistry (LAPC), Institute of Atmospheric Physics, Chinese Academy of Sciences, Beijing, 100029, China
[7]Institute of Tropical and Marine Meteorology/Guangdong Provincial Key Laboratory of Regional Numerical Weather Prediction, China Meteorological Administration, Guangzhou, 510080, China

[8]Fujian Provincial Environmental Monitoring Center, Fuzhou 350003, China
[9]Quanzhou Municipal Bureau of Meteorology, Quanzhou 361012, China
[10]Xiamen Municipal Bureau of Meteorology, Xiamen 362000, China

Received: 25 July 2015 – Accepted: 26 August 2015 – Published: 10 September 2015

Correspondence to: T. L. Zhao (tlzhao@nuist.edu.cn)

Published by Copernicus Publications on behalf of the European Geosciences Union.

ACPD
15, 24623–24642, 2015

Abstract

A high O_3 episode with the large increases in surface ozone by 21–42 ppbv and the nocturnal surface O_3 levels exceeding 70 ppbv was observed in the region between Xiamen and Quanzhou over the southeastern coast of China during 12–14 June 2014, before Typhoon Hagibis landing. Variations in the surface O_3, NO_2, CO and meteorology during Typhoon Hagibis event clearly suggest a substantial impact of the peripheral downdrafts in the large scale typhoon circulation on such an O_3 episode with excluding the contributions of photochemical production and the horizontal transport. The influence of vertical O_3 transport from the upper troposphere and lower stratosphere (UTLS) region on high surface O_3 levels is further confirmed by a negative correlation between surface O_3 and CO concentrations as well as dry surface air observed during the O_3 episode. This study provides observational evidence of typhoon-driven intrusion of O_3 from the UTLS region to surface air, revealing a significant effect of such a process of stratosphere–troposphere exchange (STE) of O_3 on tropospheric O_3 and ambient air quality.

1 Introduction

Tropospheric O_3, as an important chemical species with the effects of oxidation, toxicity and greenhouse gas on climate and environment, is generated through a series of complex photochemical reactions related to oxides of nitrogen (NO_x) and volatile organic compounds (VOC) under strong solar radiation. Both strong local photochemical production and atmospheric transport processes can lead to high surface O_3 concentrations (Jacob, 1999). Weather condition can profoundly influence tropospheric O_3 levels through physical and chemical processes and their interactions that modulate O_3 and its precursors (Huang et al., 2005; Xue et al., 2014). The variation of tropospheric O_3 is largely influenced by the STE of air mass and chemical species (Holton et al., 1995; Tang et al., 2011; Hsu and Prather, 2014).

ACPD
15, 24623–24642, 2015

A tropical cyclone (TC), as a large scale weather system with strong convection, is referred to as a typhoon over the Western Pacific or a hurricane over the Northern Atlantic. A typical TC can span a large radius of 100–2000 km with the vertical circulation of strong convection extending into the UTLS region at heights of 10–18 km (Emanuel, 1986). A three-dimensional TC circulation consists of the rotational air flow in the horizontal direction and the in-up-out-down overturning flow in the vertical direction, along which air mass near the surface can rise into thunderstorm clouds, outflowing at high levels in the UTLS and subsiding in the periphery. As an important STE mechanism, the vertical TC circulation with internal updrafts and peripheral downdrafts between the surface and the UTLS region exerts an enormous impact on air mass and energy transports in the troposphere (Baray et al., 1998; Fadnavis et al., 2011), as well as redistribution of tropospheric O_3 (Baray et al., 1999).

Air intrusions from the stratosphere to the troposphere were speculated to increase O_3 concentrations in the upper troposphere during a TC event (Bellevue et al., 2007). The uplift flows of TC also transport O_3 from the surface to the middle and upper troposphere (Fadnavis et al., 2011). Under the influence of frequent typhoon activities, O_3 episodes occurred over coastal areas in southeast China (Feng et al., 2007; Wu et al., 2013). The stagnant meteorological conditions with strong subsidence and stable stratification in the boundary layer resulted in pollutant accumulations with high O_3 before typhoon landings over southeast China (Feng et al., 2007). The peripheral O_3 was regionally transported by strong horizontal typhoon winds (Huang et al., 2006).

Convection and orographic forcing can be important for the STE and the modification of trace gases between the boundary layer and the free troposphere (Lelieveld and Crutzen, 1994; Donnell et al., 2001; Weber and Prevot, 2002; Ding et al., 2009). O_3-rich air aloft could be transported downward to the surface, when the cold front passage or nocturnal residual layer “leaky” occurred (Hu et al., 2013a, b). The near-surface O_3 levels abruptly increased by the downward O_3 from the free troposphere by tropical convections, enhancing O_3 levels in the boundary layer by as much as 20 to 30 ppbv (Betts et al., 2002; Sahu and Lal, 2006; Grant et al., 2008). A recent modeling study (Hu

ACPD
15, 24623–24642, 2015

et al., 2010) estimated that the downward transport resulted in a 39 % increase in the O_3 burden within the lower atmosphere (< 2 km) during a deep moist convection event over West Africa in August 2006. These studies on downdrafts of O_3 to the surface level are mostly focused on the mesoscale convections in the tropics. The extent to which these UTLS ozone enhancements reach the surface is poorly characterized.

Redistribution of tropospheric O_3 by the TC circulation has been studied from the perspectives of the STE of O_3, strong horizontal advection, and the stagnant meteorology for O_3 accumulations in the boundary layer. In this study, we report a new finding on the O_3-rich air downdrafts from the UTLS region to the surface driven by vertical typhoon circulation, as the deep stratospheric intrusions elevating western US of surface O_3 to unhealthy levels can be classified as "exceptional events" (Lin et al., 2015). We investigate the O_3 variation during a TC event of Typhoon Hagibis over northwest Pacific on the basis of observations of the surface air pollutants and meteorology in Xiamen and Quanzhou region (XQR) over the southeastern coast of China (Fig. 1) in June 2014. This study presents observational evidence of a surface O_3 episode caused by downward transport of O_3 in the subsiding branches of vertical TC circulation. this finding may shed some light on the function of downward O_3 transport from the UTLS/stratospheric regions in modulating O_3 in the lower troposphere with implications of the STE on air quality and climate changes.

2 Data and observation

The XQR area, a prefecture of Fujian Province, located in the western coast of Taiwan Strait, southeast China (Fig. 1). The air quality data (http://air.epmap.org/), including surface concentrations of O_3, nitrogen dioxide (NO_2) and carbon monoxide (CO), were measured at 8 environmental monitoring stations over XQR in June 2014. The surface observations of wind, air temperature, air pressure and relative humidity at the observatory of Xiamen (24.48° N, 118.07° E) were collected for meteorological analysis during Typhoon Hagibis in June 2014. The FNL meteorological data in a horizontal resolu-

ACPD
15, 24623–24642, 2015

tion of 1° × 1° with 27 vertical levels from NCEP (National Centers for Environmental Prediction, USA) are used to describe the circulations of Typhoon Hagibis.

Typhoon Hagibis, as a summertime TC over the northwest Pacific, was intensified into a strong tropical storm over the South China Sea at Dongsha islands (116.8° E, 20.6° N) and then gradually pushed northwards up the southeastern coast of China. Typhoon Hagibis made landfall in Shantou, a coastal site of Guangdong Province, south of XQR, at 16:50 (LT, same for hereinafter) 15 June with the maximum sustained winds of 23 $m\,s^{-1}$. Figure 2a–c show the distributions of sea-level pressure and near-surface wind fields over the region from southeast China to northwest Pacific at 14:00 13 June, 20:00 13 June and 20:00 15 June 2014 respectively, before and after the typhoon landing in the southeastern coast of China.

The hourly surface O_3 concentrations over XQR during Typhoon Hagibis are shown in Fig. 3a with a noticeable anomaly in O_3 concentrations before and after the typhoon landfall. XQR was situated in the typhoon periphery when Typhoon Hagibis was located in South China Sea during 12–14 June 2014 (Fig. 2a and b). A high O_3 episode occurred from the noon of 12 June to the afternoon of 14 June. In particular, the nocturnal surface O_3 concentrations exceeded 70 ppbv from 13 to 14 June 2014 (Fig. 3c). The 8 h averaged surface O_3 concentrations of 80 ppbv at Huli and Xidong (sites 5 and 6 in Fig. 1) in XQR reached the "hazardous" O_3 level of the Chinese national standards for ambient air quality. The surface O_3 abruptly decreased over XQR when Typhoon Hagibis was closer to the landfall in southeast China on 15 June 2014 (Fig. 2c). By using the hourly O_3 measurement data over XQR, the normal and anomalous patterns of diurnal O_3 changes in June 2014 and the O_3 episode could be represented with the surface O_3 concentrations averaged respectively in June excepting 12–14 June and over 12–14 June 2014 (Fig. 3d). It is shown in Fig. 3d that the normal surface O_3 levels over XQR in June 2014 shifted diurnally from 17 ppbv at 2:00 to 52 ppbv at 14:00 with a daily O_3 mean of about 30 ppbv, while the anomalously high surface O_3 levels during the O_3 episode varied between nighttime 51 ppbv and daytime 70 ppbv with an O_3 mean of about 57 ppbv. Comparing to the normal O_3 levels in June 2014, the av-

ACPD
15, 24623–24642, 2015

eraged enhancements of surface O_3 by about 21 ppbv in daytime and up to 42 ppbv in nighttime over XQR are estimated for the O_3 episode before Typhoon Hagibis landing.

3 Analysis and discussion

The surface O_3 variation is complex, resulted from interactions of chemical production and dynamic transport on different scales (Jacob, 1999). In the following we examine this case of surface O_3 peak before a typhoon landing in southeast China from chemical production, horizontal advection and vertical transport.

Tropospheric O_3 is produced through a series of complex photochemical reactions of NO_x and VOC under strong solar radiation. The O_3 concentrations in suburban and rural areas are usually most sensitive to NO_x variations (Chameides et al., 1992; Duncan and Chameides, 1998). Notably, the surface NO_2 levels kept around 10 ppbv during the O_3 episode from 12 to 14 June, almost the same as normal NO_2 levels during non-polluted days (Fig. 3b and c). In particularly high O_3 levels anomalously persisted in the night without photochemical reaction. Therefore, photochemical production could not be speculated to determine the high O_3 episode. Furthermore, any obvious increases in surface air temperature were not observed for strong photochemical reactions for such high O_3 production during the episode of 12–14 June in XQR (Fig. 4a), since air temperature could represent the solar radiation conditions during summertime. As we know, the weather is characterized by the clear sky, strong solar radiation, weak wind, and stable atmospheric boundary layer when TC is about 600 to 1000 km away. All these are the favorable conditions for photochemical production of O_3, which is confirmed by the diurnal variation of O_3 during the episode (Fig. 3d), However, a comparison of diurnal O_3 changes in June 2014 and during the O_3 episode (Fig. 3d) clearly presents the anomalies in the diurnal O_3 variation over 12–14 June, suggesting a less contribution of the local photochemical O_3 production to the peak O_3.

During 12–14 June, weak easterly winds over XQR (Figs. 2a and 4b) were observed to be unfavorable for horizontal transport of O_3 and its precursors. The easterly wind

ACPD
15, 24623–24642, 2015

could even carry clean air from the Pacific Ocean to XQR. Moreover, the daily change of near-surface air mass divergence over XQR clearly presented a shift of the negative to positive values for convergence and divergence conditions during normal and high O_3 periods (Fig. 3b). The near-surface air mass divergence (positive values in divergence in Fig. 4b) in association with a high surface air pressure (Fig. 4c) over XQR suppressed the advection import O_3 and its precursors towards XQR during the O_3 episode of 12–14 June 2014. The meteorological conditions of easterly clean air from ocean and near-surface air divergence over XQR were unfavorable to horizontal transport of air pollutants to XQR during the O_3 episode. Therefore, the surface O_3 peak of 12–14 June before the typhoon landing was unlikely caused by horizontal advection or transport of O_3 and its precursors.

Figures 5 presents the cross sections of vertical velocity along the lines from the typhoon center to XQR (as shown in Fig. 2 with the black solid lines) at 14:00 and 20:00 13 June, as well as 20:00 15 June 2014 respectively. In accompany with the strong rising motions from the surface up to the UTLS around 100 hPa near the typhoon center (Fig. 5a and b), the subsiding branches of vertical typhoon circulation were located over XQR in the northeastern periphery of Typhoon Hagibis at 14:00 and 20:00 13 June 2014 (Figs. 2a, b and 5a, b). A typical structure of TC circulation with the in-up-out-down overturning flows in the vertical direction built up the internal updrafts and peripheral downdrafts for air mass exchange between the surface level and the UTLS region (Fig. 5a and b). The deep and strong downdrafts occurred over XQR (24° N, 118° E) during this episode before the typhoon landfall. As Typhoon Hagibis approached and landed the coast in southeast China (Fig. 2), the downdrafts were changed to the updrafts over XQR on 15 June (Fig. 5c), and the surface O_3 concentrations dropped to the normal levels over XQR (Fig. 3a).

A climatological pattern of vertical O_3 distribution presents the uniquely elevated O_3 concentrations in the UTLS region (Liu et al., 2013). The large scale convections of Typhoon Hagibis were fully developed and well organized with strong uplifts reaching to the UTLS around 100 hPa and consecutively downward flows to the surface level

ACPD
15, 24623–24642, 2015

over XQR (Fig. 5a and b), which could efficiently deliver O_3-rich air from the UTLS region to the surface leading to the surface O_3 enhancement by about 27 ppbv in daytime and up to 40 ppbv in nighttime observed over XQR during 12–14 June (Fig. 3c and d). Furthermore, low relative humidity and high air pressure on the XQR surface during 12–14 June (Fig. 4c and d) add evidences for the strong downward transport of O_3 in the subsiding branches of TC with dry air mass of the UTLS region affecting the surface air, given that surface relative humidity dropped sharply (Fig. 4d) and air temperature decreased slightly (Fig. 4a) over XQR during 12–14 June. Therefore, it is the downdrafts of O_3-rich air from the UTLS that played a decisive role in the formation of O_3 episode before a typhoon landing in southeast China.

The correlation between O_3 and CO has been widely used to identify sources of tropospheric O_3. When O_3 and CO are positively correlated, O_3 is usually originated from the anthropogenic sources with photochemical reactions (Parrish et al., 1998; Voulgarakis et al., 2011). A negative correlation of O_3 and CO generally indicates the vertical O_3 transport from the upper atmosphere, where air is poor in CO but rich in O_3 (Moody et al., 1995; Parrish et al., 1998). The correlations between hourly CO and O_3 concentrations measured at 8 sites in XQR are shown over two periods from 12:00 11 June to 12:00 12 June and from 12:00 13 June to 12:00 14 June, respectively (Fig. 6). In contrast to a significantly positive correlation of the CO and O_3 during the first period, reflecting a dominant role of anthropogenic sources in the O_3 changes (Fig. 6a), the CO and O_3 concentrations were negatively correlated (significantly at $P < 0.005$) during the second period (Fig. 6b), further confirming that the O_3 episode with nocturnal high O_3 over XQR was largely contributed by downward transport of O_3-rich air in the peripheral subsidence of Typhoon Hagibis. For interpreting the higher CO concentrations during the O_3 episode (Fig. 6b) comparing to the CO levels before the O_3 episode (Fig. 6a), we may consider the atmospheric removal of CO by hydroxyl radical (OH). It is well-known that O_3 photolysis produces O^1d, which react with H_2O to produce 2OH, and the reaction of CO with OH quickly forms the stable end product of carbon dioxide (CO_2) (Seinfeld and Spyros, 2006). In the situation of normal photochemical production

ACPD
15, 24623–24642, 2015

(Fig. 6a), high O_3 could lead to more OH production and consequently lower CO. In the situation of peripheral O_3-rich air subsidence of the typhoon, the downward dry air (Fig. 4d) with lower abundance of OH radicals could decrease the removal of CO. This would result in CO accumulation and consequently high CO concentrations, and high CO accumulation within boundary layer could overwhelm the dilution of CO-poor air from the UTLS during the high O_3 episode.

4 Summary

This observation study presents an O_3 episode due to downward transport from the UTLS to surface air in the peripheral TC subsidence over the southeastern coast of China. An exceptionally high O_3 event during 12–14 June 2014 was observed with the nocturnal surface O_3 levels exceeding 70 ppbv and large enhancements of surface O_3 concentrations by about 21 ppbv in daytime and up to 42 ppbv in nighttime. The ground observations of O_3, NO_2 and CO accompanying meteorology from both observations and reanalysis over XQR during the event of Typhoon Hagibis are examined to assess the contributions of chemical production, horizontal advection and vertical transport to the O_3 episode.

As the contributions of horizontal advection and chemical production to surface O_3 enhancement in the O_3 episode are excluded, the peripheral subsiding branches in the TC circulation bringing O_3-rich air from the UTLS to surface air are identified to be responsible for peaking the surface O_3 levels over the southeastern coast of China during 12–14 June 2014 before the landfall of Typhoon Hagibis. This rational analysis is further supported by a significantly negative correlation between the surface O_3 and CO as well as the dry surface air observed during the O_3 episode.

This case study of Typhoon Hagibis provides observational evidence of TC-driven vertical transport of O_3 from the UTLS region to the surface, revealing a significant effect of such a process of STE of O_3 on deterioration of air quality. Evidence suggests deep stratospheric intrusions can elevate surface O_3 to unhealthy levels before

ACPD
15, 24623–24642, 2015

a typhoon landing in southeast China. Stratospheric O_3 is a natural source dominating tropospheric O_3 pollution in this scenario. Considering the frequency and distribution of TC in the world and their impact on STE, this finding has implications on tropospheric O_3 as well as environment and climate changes.

A pattern of well-organized deep TC convection for the exchange of chemical species between the UTLS and surface air is depicted in this case study of TC in southeast China. Based on the understanding of the dynamical structure of TC and the chemical distribution in the atmosphere, the strong subsiding branches of vertical TC circulation could unusually transport the upper O_3-rich air to the surface in any TC events, which is to be further studied with more comprehensive observations to characterize the extent to which these UTLS ozone enhancements reach the surface. The implications of this finding on environment and climate changes need to be explored by using coupled meteorology-chemistry models.

Acknowledgements. This work was jointly funded by National Science and Technology Project of China (2014BAC22B04), the Key Basic Research Program of China (2014CB441203), the Science and Technology Support Program of Jiangsu Province, China (BE2 012 771) and National Natural Science Foundation of China (40 906 023). The air quality data were obtained freely from the Chinese Ministry of Environmental Protection (http://air.epmap.org/). The NCEP-FNL meteorological data were freely downloaded from the NOAA-CIRES Climate Diagnostics Center, Boulder, Colorado, USA (http://rda.ucar.edu/datasets/).

References

Baray, J. L., Ancellet, G., Taupin, F. G., Bessafi, M., Baldy, S., and Keckhut, P.: Subtropical tropopause break as a possible stratospheric source of ozone in the tropical troposphere, J. Atmos. Sol.-Terr. Phy., 60, 27–36, doi:10.1016/S1364-6826(97)00116-8, 1998.

Baray, J. L., Ancellet, G., Randriambel, T., and Baldy, S.: Tropical cyclone Marlene and stratosphere–troposphere exchange, J. Geophys. Res., 104, 13953–13970, doi:10.1029/1999JD900028, 1999.

Bellevue, J., Baray, J. L., Baldy, S., Ancellet, G., Diab, R. D., and Ravetta, F.: Simulations of stratospheric to tropospheric transport during the tropical cyclone Marlene event, Atmos. Environ., 41, 6510–6526, doi:10.1016/j.atmosenv.2007.04.040, 2007.

Betts, A. K., Gatti, L. V., Cordova, A. M., Silva Dias, M. A. F., and Fuentes, J. D.: Transport of ozone to the surface by convective downdrafts at night, J. Geophys. Res., 107, 8046, doi:10.1029/2000JD000158, 2002.

Chameides, W. L., Fehsenfeld, F., Rodgers, M. O., Cardelino, C., Martinez, J., Parrish, D., Lonneman, W., Lawson, D. R., Rasmussen, R. A., Zimmerman, P., Greenberg, J., Middleton, P., and Wang, T.: Ozone precursors relationships in the ambient atmosphere, J. Geophys. Res., 97, 6037–6055, doi:10.1029/91JD03014, 1992.

Ding, A., Wang, T., Xue, L., Stohl, A., Lei, H., Jin, D., Ren, Y., Wang, X., Wei, X., Qi, Y., Liu, J., and Zhang, X.: Transport of north China air pollution by midlatitude cyclones: case study of aircraft measurements in summer 2007, J. Geophys. Res., 114, D08304, doi:10.1029/2008JD011023, 2009.

Donnell, E. A., Fish, D. J., Dicks, E. M., and Thorpe, A. J.: Mechanisms for pollutant transport between the boundary layer and the free troposphere, J. Geophys. Res., 106, 7847–7856, doi:10.1029/2000JD900730, 2001.

Duncan, B. N. and Chameides, W. L.: Effects of urban emission control strategies on the export of ozone and ozone precursors from the urban atmosphere to the troposphere, J. Geophys. Res., 103, 28159–28179, doi:10.1029/98JD02145, 1998.

Emanuel, K. A.: An air–sea interaction theory for tropical cyclones, Part I: Steady-state maintenance, J. Atmos. Sci., 43, 585–605, doi:10.1175/1520-0469(1986)043<0585:AASITF>2.0.CO;2, 1986.

Fadnavis, S., Berg, G., Buchunde, P., Ghude, S. D., and Krishnamurti, T. N.: Vertical transport of ozone and CO during super cyclones in the Bay of Bengal as detected by Tropospheric Emission Spectrometer, Environ. Sci. Pollut. R., 18, 301–315, doi:10.1007/s11356-010-0374-3, 2011.

Feng, Y., Wang, A., Wu, D., and Xu, X.: The influence of tropical cyclone Melor on PM_{10} concentrations during an aerosol episode over the Pearl River Delta region of China: numerical modeling versus observational analysis, Atmos. Environ., 41, 4349–4365, doi:10.1016/j.atmosenv.2007.01.055, 2007.

Grant, D. D., Fuentes, J. D., DeLonge, M. S., Chan, S., Joseph, E., Kucera, P., Ndiaye, S. A., and Gaye, A. T.: Ozone transport by mesoscale convective storms in western Senegal, Atmos. Environ., 42, 7104–7114, doi:10.1016/j.atmosenv.2008.05.044, 2008.

Holton, J. R., Haynes, P. H., McIntyre, M. E., Douglass, A. R., Rood, R. B., and Pfister, L.: Stratosphere–troposphere exchange, Rev. Geophys., 33, 403–439, 1995.

Hsu, J. and Prather, M. J.: Is the residual vertical velocity a good proxy for stratosphere–troposphere exchange of ozone?, Geophys. Res. Lett., 41, 9024–9032, doi:10.1002/2014GL061994, 2014.

Hu, X. M., Fuentes, J. D., and Zhang, F.: Downward transport and modification of tropospheric ozone through moist convection, J. Atmos. Chem., 65, 13–35, doi:10.1007/s10874-010-9179-5, 2010.

Hu, X. M., Klein, P. M., Xue, M., Shapiro, A., and Nallapareddy, A.: Enhanced vertical mixing associated with a nocturnal cold front passage and its impact on near-surface temperature and ozone concentration, J. Geophys. Res., 118, 2714–2728, doi:10.1002/jgrd.50309, 2013a.

Hu, X. M., Klein, P. M., Xue, M., Zhang, F., Doughty, D. C., Forkel, R., Joseph, E., and Juentes, J. D.: Impact of the vertical mixing induced by low-level jets on boundary layer ozone concentration, Atmos. Environ., 70, 123–130, doi:10.1016/j.atmosenv.2012.12.046, 2013b.

Huang, J. P., Fung, C. H., Lau, K. H., and Qin, Y.: Numerical simulation and process analysis of typhoon-related ozone episodes in Hong Kong, J. Geophys. Res., 110, D05301, doi:10.1029/2004JD004914, 2005.

Huang, J. P., Fung, C. H., and Lau, K. H.: Integrated processes analysis and systematic meteorological classification of ozone episodes in Hong Kong, J. Geophys. Res., 111, D20309, doi:10.1029/2005JD007012, 2006.

Jacob, D. J.: Introduction of Atmospheric Chemistry, Princeton Univ. Press, Princeton, NJ, 234–243, 1999.

Lelieveld, J. and Crutzen, P. J.: Role of deep cloud convection in the ozone budget of the troposphere, Science, 264, 793–797, 1994.

Lin, M., Fiore, A. M., Horowitz, L. W., Langford, A. O., Oltmans, S. J., Tarasick, D., and Rieder, H. E.: Climate variability modulates western US ozone air quality in spring via deep stratospheric intrusions, Nature, 6, 7105, doi:10.1038/ncomms8105, 2015.

Liu, J., Tarasick, D. W., Fioletov, V. E., McLinden, C., Zhao, T., Gong, S., Sioris, C., Jin, J. J., Liu, G., and Moeini, O.: A global ozone climatology from ozone soundings via trajectory map-

ping: a stratospheric perspective, Atmos. Chem. Phys., 13, 11441–11464, doi:10.5194/acp-13-11441-2013, 2013.
Moody, J. L., Oltmans, J., and Merrill, T.: Transport climatology of tropospheric ozone: Bermuda, 1988–1991, J. Geophys. Res., 100, 7179–7194, doi:10.1029/94JD02830, 1995.
Parrish, D. D., Trainer, M., Holloway, J. S., Yee, J. E., Warshawsky, M. S., Fehsenfeld, F. C., Forbes, G. L., and Moody, J. L.: Relationships between ozone and carbon monoxide at surface sites in the North Atlantic region, J. Geophys. Res., 103, 13357–13376, 1998.
Sahu, L. K. and Lal, S.: Changes in surface ozone levels due to convective downdrafts over the Bay of Bengal, Geophys. Res. Lett., 33, L10807, doi:10.1029/2006GL025994, 2006.
Seinfeld, J. H. and Spyros, N. P.: Atmospheric Chemistry and Physics: From Air Pollution to Climate Change, 2nd edn., J. Wiley, New York, 2006.
Tang, Q., Prather, M. J., and Hsu, J.: Stratosphere–troposphere exchange ozone flux related to deep convection, Geophys. Res. Lett., 38, L03806, doi:10.1029/2010GL046039, 2011.
Voulgarakis, A., Telford, P. J., Aghedo, A. M., Braesicke, P., Faluvegi, G., Abraham, N. L., Bowman, K. W., Pyle, J. A., and Shindell, D. T.: Global multi-year O_3-CO correlation patterns from models and TES satellite observations, Atmos. Chem. Phys., 11, 5819–5838, doi:10.5194/acp-11-5819-2011, 2011.
Weber, R. O. and Prevot, A. S. H.: Climatology of ozone transport from the free troposphere into the boundary layer south of the Alps during North Foehn, J. Geophys. Res., 107, 4030, doi:10.1029/2001JD000987, 2002.
Wu, M., Wu, D., Fan, Q., Wang, B. M., Li, H. W., and Fan, S. J.: Observational studies of the meteorological characteristics associated with poor air quality over the Pearl River Delta in China, Atmos. Chem. Phys., 13, 10755–10766, doi:10.5194/acp-13-10755-2013, 2013.
Xue, L. K., Wang, T., Gao, J., Ding, A. J., Zhou, X. H., Blake, D. R., Wang, X. F., Saunders, S. M., Fan, S. J., Zuo, H. C., Zhang, Q. Z., and Wang, W. X.: Ground-level ozone in four Chinese cities: precursors, regional transport and heterogeneous processes, Atmos. Chem. Phys., 14, 13175–13188, doi:10.5194/acp-14-13175-2014, 2014.

ACPD
15, 24623–24642, 2015

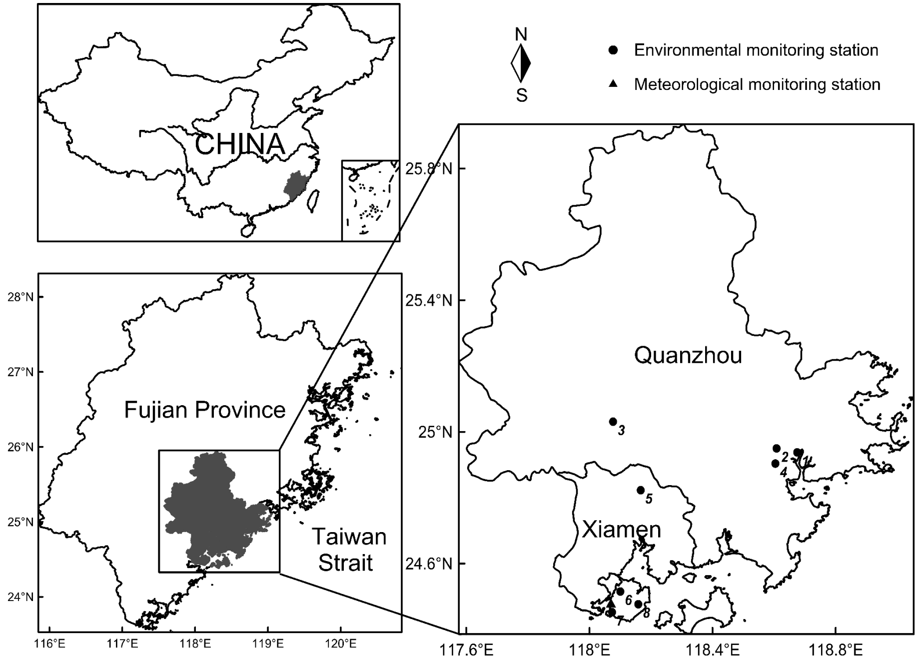

Figure 1. Locations of Fujian Province in China (shaded areas, upper left panel) and the Xiamen and Quanzhou region (XQR) in Fujian Province (shaded areas, lower left panel), and the distribution of 9 monitoring stations (8 environmental sites with black dots numbering from 1 to 8, and 1 meteorological observatory of Xiamen with a black triangle) over XQR (lower right panel).

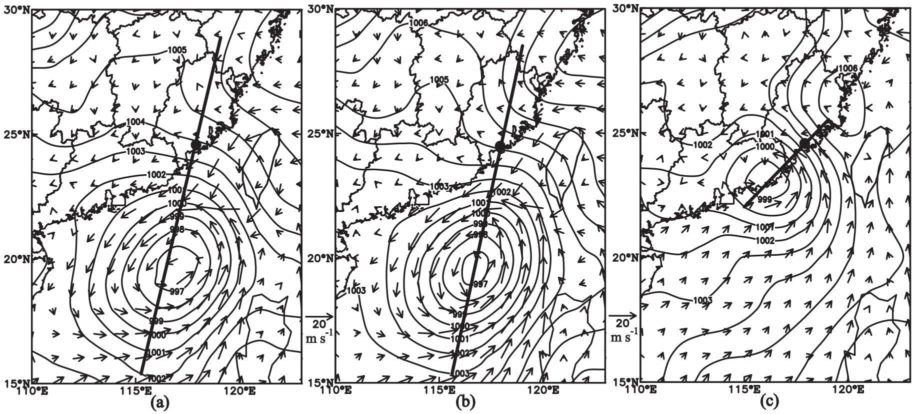

Figure 2. Sea-level air pressure (hPa, contour lines) and 1000 hPa wind vectors of NCEP-FNL data, at **(a)** 14:00 13 June, **(b)** 20:00 13 June and **(c)** 20:00 15 June 2014 with black dots representing XQR location. Three straight lines link XQR and the centers of Typhoon Hagibis.

ACPD
15, 24623–24642, 2015

Why does surface ozone peak before a typhoon landing in southeast China?

Y. C. Jiang et al.

Title Page
Abstract | Introduction
Conclusions | References
Tables | Figures
◀ | ▶
◀ | ▶
Back | Close
Full Screen / Esc
Printer-friendly Version
Interactive Discussion

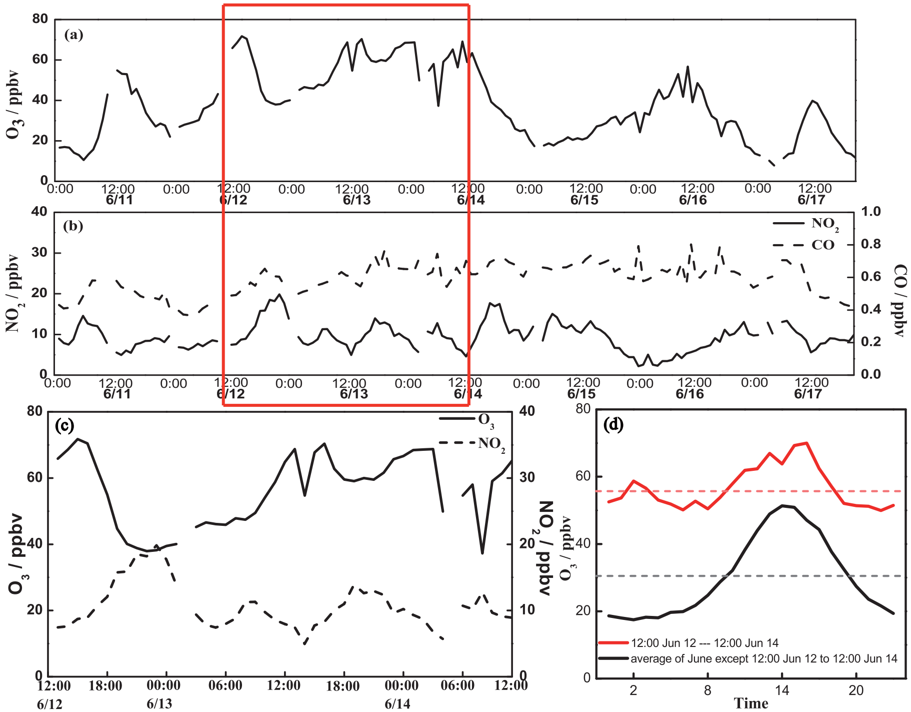

Figure 3. Hourly variations in the 8-site averaged surface concentrations of **(a)** O_3,**(b)** NO_2 during 11–17 June and **(c)** O_3 and NO_2 for the surface O_3 event during 12–14 June 2014 over XQR, as well as **(d)** diurnal changes of surface O_3 from 12:00 June 12 to 12:00 June 14 (red curve) and in June excluding 12–14 June 2014 (black curve) with two dotted lines indicating the daily averaged O_3 concentrations for two diurnal curves.

ACPD

15, 24623–24642, 2015

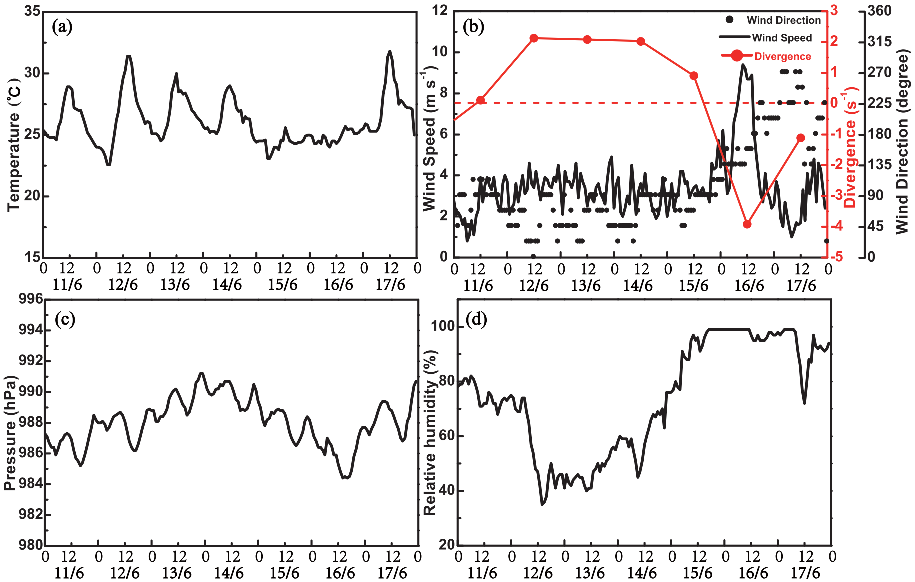

Figure 4. Time series of **(a)** surface air temperature as well as **(b)** wind speed, direction and divergence, **(c)** air pressure and **(d)** relative humidity observed in the observatory of Xiamen from 11 to 17 June 2014. The red curve in **(b)** is a daily variation in divergences at 1000 hPa over XQR, calculated with FNL data.

ACPD
15, 24623–24642, 2015

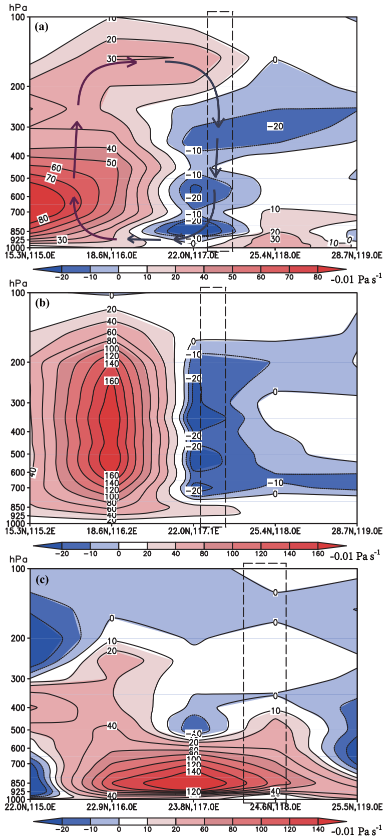

Figure 5. Vertical cross sections of vertical velocity ($-0.01\,\mathrm{Pa\,s^{-1}}$) along the three straight lines linking XQR and the centers of Typhoon Hagibis in Fig. 2 at **(a)** 14:00 13 June, **(b)** 20:00 13 June and **(c)** 20:00 15 June 2014 (FNL data). Two dash boxes denote the location of XQR. The lines with arrows indicate the in-up-out-down overturning air flows in the vertical direction of typhoon.

ACPD
15, 24623–24642, 2015

Why does surface ozone peak before a typhoon landing in southeast China?

Y. C. Jiang et al.

Title Page
Abstract | Introduction
Conclusions | References
Tables | Figures
◄ | ►
◄ | ►
Back | Close
Full Screen / Esc
Printer-friendly Version
Interactive Discussion

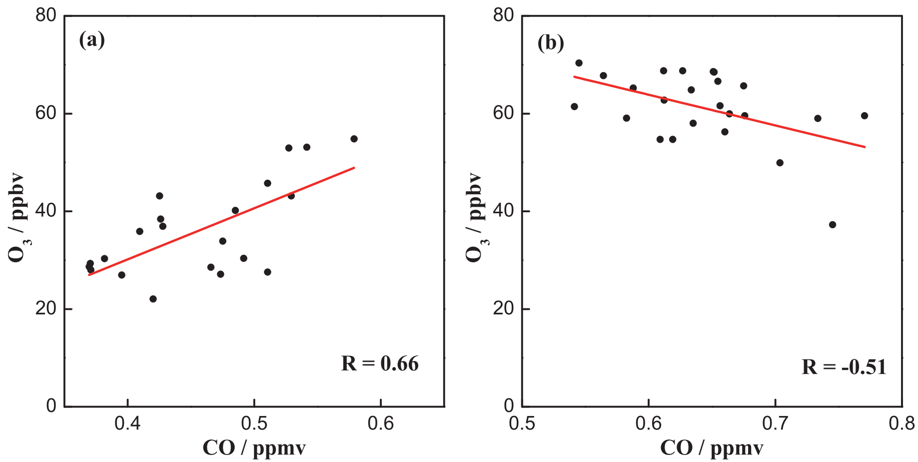

Figure 6. Correlations between measured surface CO and O_3 over two periods respectively **(a)** from 12:00 11 June to 12:00 12 June and **(b)** from 12:00 13 June to 12:00 14 June 2014, passing the significant level of 0.005. Red lines are the linear fittings.

ACPD
15, 24623–24642, 2015

Why does surface ozone peak before a typhoon landing in southeast China?

Y. C. Jiang et al.